Loop-Star Decomposition of Basis Functions in the Discretization of the EFIE

Giuseppe Vecchi, *Member, IEEE*

***Abstract*— A general and readily applicable scheme is presented for the determination of the basis functions that allow the decomposition of the surface current into a solenoidal part and a nonsolenoidal remainder. The proposed approach brings into correspondence these two parts with two scalar functions and generates the known loop and star basis functions. The completeness of the loop-star basis is discussed, employing the presented scheme; the issue of the irrotational property of the nonsolenoidal functions is addressed.**

***Index Terms*— EFIE, loops, planar circuits, printed antennas, scattering, stars.**

I. Introduction

In the electric-field integral equation (EFIE) for conducting bodies, the choice of suitable basis functions to represent the approximate solution is obviously an important point. In the general case of a surface of arbitrary shape, in addition to specific constraints on individual vector basis functions [1], the necessity for a correct representation of the solenoidal part of the solution (surface current) has emerged from different works and viewpoints. A very good survey of recent advances in this sense can be found in two similar papers [2], [3], that also credit the originating works. The issue originated from the need to avoid the "low-frequency catastrophe" associated with the extreme bad conditioning that the numerical problem assumes when approaching static or quasi-static conditions on a large and geometrically complex structure; this occurrence can be avoided by separating the solenoidal part of the current. A historical perspective of the earlier works is found in [3], which will be taken as reference in the following; an early contribution on the subject is also found in [4], while partial application to printed antennas appeared in [5].

The solution of an EFIE problem has to be *div-conforming* [1], i.e., able to represent a zero-divergence current field; equivalently, a set of basis functions has to be found that completely represents the solenoidal part of the solution. This is usually done by recognizing that solenoidal currents form closed paths, which has led to the introduction of *loop*-type basis functions [3]. Identification of the solenoidal part brings to attention the dual, equally important issue of finding a basis that spans the remaining nonsolenoidal part of the initial space spanned by the chosen (vector) basis functions. In the literature, this has led either to the tree and co-tree strategies, or to the introduction of the so-called "star" basis functions [3], [6].

While the present issue is of recognized importance in the context of low-frequency analysis, it can be noted that "low-frequency" is equivalent to near-field behavior and the latter is the main responsible of the the growth of the condition number for increasing number of unknowns when studying complex structures like planar antennas and circuits [7] at their normal frequency of operation. This need has also expanded to the issue of correctly representing the singular part of the EFIE that is crucial in obtaining a proper solution [7]–[9].

This loop-star decomposition has also been the subject of a more recent work [10] in which the functions of the "star" basis of [4] are instead termed "patch" functions.

As to this remainder nonsolenoidal subspace, contrary to intuition, the word "irrotational" is improper and to some extent misleading, as detailed in Sections III and IV; therefore, this labeling of the nonsolenoidal subspace will not be employed in the following.

Application of the loop-star basis has been described in connection to metal scatterers [2], [3] and in connection with the analysis of planar printed antennas [8]–[11] and the properties of the EFIE in this basis have been discussed in [7] and [8]; this paper will not be concerned with the use of this basis in specific problems, but rather on the *generation* and properties of the loop-star representation itself.

The procedures described in this paper afford a systematic way of generating these dual bases and assess the completeness of the representation with respect to the usual discretization of the solution. To the best of the author's knowledge this information is missing in the available literature.

In this paper, a conductor of arbitrary shape will be considered (with surface Σ) onto which the solution to the EFIE problem is represented by N vector basis functions defined over a triangular or rectangular mesh with N_c cells denoted by Σ_a, $a = 1 : N_c$. The position on the surface Σ will be denoted by $\underline{\rho}$ and the surface current by $\underline{J}(\underline{\rho})$; the unknown $\underline{J}$ will be represented by the simplest meaningful vector basis functions [12], precisely termed "zeroth order Nedelec" in [1], and here dubbed by their widespread name of "rooftops" and denoted by $\underline{R}_n$,

$$\underline{J}(\underline{\rho}) = \sum_{n=1}^{N} I_n \underline{R}_n(\underline{\rho}) \tag{1}$$

where the number N of rooftop functions equals the number of inner edges of the mesh [1]. This work addresses the issue of generating the basis functions for the solenoidal part $\underline{J}''$

Manuscript received December 25, 1997; revised July 15, 1998.

The author is with the Dipartimento di Elettronica, Politecnico, I-10129 Torino, Italy.

Publisher Item Identifier S 0018-926X(99)03716-3.

0018–926X/99$10.00 © 1999 IEEE

and for the nonsolenoidal remainder $\underline{J}'$ of the space spanned by the rooftops $\underline{J} = \underline{J}' + \underline{J}''$. A procedure is adopted that has the advantage of easily generating these functions on any mesh; this will allow to obtain the usual "loop" and "star" groupings of rooftops, but at the same time establishing a more general frame that seems well suited for finding more efficient bases and, notably, for the multilevel/multiresolution analysis. Preliminary work in this sense is described in [13]; generation of multiresolution bases is, however, outside the scope of this paper and will be addressed elsewhere.

The basis functions for the solenoidal and nonsolenoidal subspaces will be linear combinations of the initial shape-conforming rooftops $\underline{R}_n$ subject to the condition that the mesh be able to close all loops. At any (regular) point on the metal surface Σ, the normal direction is denoted by $\hat{n}$ and $\hat{\tau}_1$ and $\hat{\tau}_2$ are the two orthogonal directions tangent to the surface $\hat{\tau}_1 \times \hat{\tau}_2 = \hat{n}$. In the following, the subscript t will refer to surface coordinates ("tangential") and the surface divergence and curl of the surface current are expressed through the surface grad operator $\nabla_t = \nabla - \hat{n}(\partial/\partial n)$.

Summarizing the strategy, the goal is to find a new basis that: 1) explicitly contains the solenoidal functions and 2) is equivalent to the original rooftop basis. Therefore, one first needs an "algorithm" to specify the loop (solenoidal) basis and then another "algorithm" to specify a basis for the remaining nonsolenoidal part of the space in such a way that the two bases are globally equivalent to the rooftop basis, i.e., able to represent all functions $\underline{J}$ that are linear combinations of rooftops.

II. Solenoidal Part

A. Generation via Scalar Functions

Since the chosen basis for $\underline{J}$ has to be div-conforming, the solenoidal condition $\nabla_t \cdot \underline{J}'' = 0$ holds everywhere, which, in turn, implies that

$$\underline{J}''(\underline{\rho}) = \nabla_t \times \hat{n} M(\underline{\rho}), \quad \nabla_t \cdot \underline{J}'' = 0, \quad \forall \underline{\rho} \in \Sigma \qquad (2)$$

Therefore, this part of the current is represented by a scalar function M and the solenoidal basis functions are naturally derived from those chosen for M. Apart for a constant, M is the normal magnetic current [7]; because of its meaning in (2), here M will be referred to as "solenoidal potential." The regularity condition for the rooftops [1] directly translates into the requirement for M to be piecewise linear. As a result, the natural representation for the scalar function M is based on the *nodes* of the mesh; the basic and simplest choice is to employ the scalar linear Lagrange (or nodal interpolating) basis, i.e., the piecewise linear functions $\Lambda_\alpha(\underline{\rho})$ with support on the cells that have a vertex at the αth node of the mesh, attaining a unit value at node α, and linearly going to zero on all neighboring nodes. In a rectangular mesh, each rooftop extends over two rectangular cells of the mesh and the Lagrange basis functions are "pyramids" over a rectangle formed by four adjacent cells. In a triangular mesh, the rooftops still extend over pairs of cells with one common edge, but in an unstructured mesh the number of cells around each node depends on the local

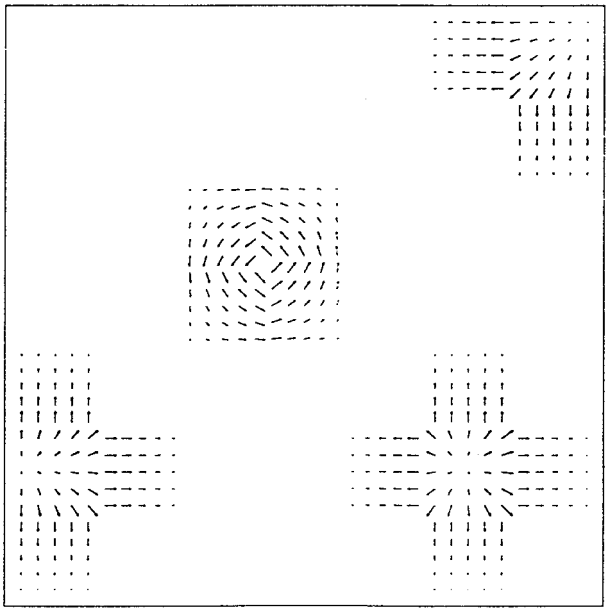

Fig. 1. Loop-star grouping of rooftop-basis functions for the case of a rectangular mesh. A loop $\underline{L}(\underline{\rho})$ composed of four rooftops is shown in the middle; the others are star functions $\underline{X}(\underline{\rho})$, and show the deformation of stars when at the boundary.

properties of the triangulation; the scalar functions Λ_α will be "teepee-like tents" over the polygonal region surrounding each node α. The curl operation in (2)

$$\underline{L}_\alpha(\underline{\rho}) = \nabla_t \times \hat{n} \Lambda_\alpha(\underline{\rho}) \qquad (3)$$

will generate basis functions representing closed current loops on the polygonal region, circulating around node α. These loop-basis functions will be denoted by $\underline{L}(\underline{\rho})$ in the following, i.e.,

$$\underline{J}''(\underline{\rho}) = \sum_\alpha I''_\alpha \underline{L}_\alpha(\underline{\rho}). \qquad (4)$$

For the sake of illustration, the case of loops in a rectangular mesh is shown in Fig. 1; loops and stars on a triangular mesh are shown in [2] and [3]. Note that for a flat surface, $\nabla_t \times \hat{n} M(\underline{\rho}) = \hat{n} \times \nabla_t M$.

The connection between the solenoidal current and a "potential" function M, which is a scalar, allows one to determine the number of basis functions necessary to represent $\underline{J}''$ for the chosen discretization. Since the current has to be zero outside the surface, the scalar function M has to be constant outside the considered surface Σ as well as over the regions representing holes in Σ (if it is not simply connected) and has to attain the same constant value at all nodes bordering the contour $\Gamma = \partial\Sigma$ of Σ. This contour is the union of the outer boundary Γ_o and the contours γ_i bordering the N_H inner holes (if any), $\Gamma = \Gamma_o \bigcup \{\bigcup_{i=1}^{N_H} \gamma_i\}$ and the above considerations are equivalent to stating that there is one extra current loop around the outer boundary Γ_o and N_H extra loops circling the inner holes. It remains to ascertain whether they are necessary or not to represent the solenoidal current. Beginning with the simply connected case (no holes, $N_H = 0$), one can observe that the outermost loop along the external boundary Γ_o can be represented by the inner loop functions in the following

manner. One sums up all the inner loops that touch the external boundary Γ_o, obtaining the outermost loop and an adjacent, counterlooping current path; since this latter does not touch the contour Γ_o, it can be represented by the inner loops (it is represented by a potential that vanishes at the boundary Γ_o) and, therefore, by subtracting this linear combination of inner loop functions one obtains the outermost boundary loop. As a result, this latter is not a linearly independent function of the solenoidal space, the constant outer potential is not a degree of freedom and it can be set to any constant value (zero, for simplicity). Therefore, on a simply connected surface $(N_H = 0)$, the number N_ℓ of necessary basis functions for the solenoidal part is equal to the number of internal nodes of the mesh; that is, the number of nodes necessary to specify the scalar function M via the linear interpolatory basis functions Λ. If there is a hole $(N_H = 1)$, when the outermost boundary loop is represented by inner loops, a counterflowing loop appears around the hole. In this case, it is therefore necessary to add a function that represents either one of the two boundary loops (which makes the other representable by inner loops); for simplicity, one can choose to add the boundary loop around the hole, requiring the constant potential over the hole to be a degree of freedom. Similarly, for a general multiply connected surface Σ $(N_H \geq 1)$, one needs N_H extra basis functions, representing loops bounding the holes or, equivalently, the generating "flat-top" linear scalar potential functions having constant value on the nodes around the hole and going to zero on neighboring inner nodes. The same prescription was obtained in [4] on the basis of topological considerations.

Note that the loops $\underline{L}_\alpha$ defined above are the smallest loops that one can define; any set of functions $M_i(\underline{\rho}) = \sum_{i=1}^{N_\ell} \mu_{i\alpha}\Lambda_\alpha(\underline{\rho})$ obtained by independent linear combinations of the elementary scalar functions Λ can be employed, generating, in turns, current loops $\underline{J}_i''(\underline{\rho})$ via (2), having shapes that can better fit the solution of specific problems.

B. Differential Properties of Loops

It can be observed that testing the (purely normal) curl $\nabla_t \times \underline{J}$ of any function over a set of weight function ϕ_k and integrating by parts (i.e., applying Green's lemma) the inner product, one obtains

$$\langle \phi_k, \hat{n} \cdot \nabla_t \times \underline{J} \rangle = \langle \underline{\psi}_k, \underline{J} \rangle, \qquad \underline{\psi}_k = \nabla_t \times \hat{n}\phi_k. \quad (5)$$

Hence, it is apparent that testing ("measuring") the curl of the current is equivalent to projecting it onto a set of solenoidal functions $\underline{\psi}_k$. The first observation that follows is that on a perfectly electrical conducting (PEC) surface, testing the EFIE on the loop functions is equivalent to enforcing the boundary condition via the normal magnetic field component; this was already observed in [7] and [8]. The second observation is that the loop functions $\underline{L}_k(\underline{\rho}) = \nabla_t \times \hat{n}\Lambda_k(\underline{\rho})$ act as a discretized version of the curl operator, yielding (upon testing) the averaged value of the curl of a function over the loop domain.

III. Nonsolenoidal Complement

As stated in the Introduction, having found a basis for the solenoidal part, one now needs to find a complementary basis that taken together with the loop basis constitutes a complete basis for the solution $\underline{J}$; that is, one must specify the $N_x \equiv N - N_\ell$ basis functions $\underline{X}_n$ for the nonsolenoidal remainder $\underline{J}'$. The intuitive guidelines arise from the duality with respect to the loop basis and specifically that: 1) the divergence of the sought-for functions is never identically zero and 2) these functions should operate as the discretized version of the div operator (since loops act as a discretized curl). These intuitive guidelines will be implemented into a systematic scheme and the first step in the procedure for finding this complementary basis is the definition of the properties of such a basis.

A. Definition of Requirements

While the property dual to div free is curl free, the discretizing basis (rooftops) for the representation of the EFIE solution must be div conforming and this makes it impossible for the basis to be also curl conforming [1] (this is detailed further in Section III-D). Therefore, in constructing a new basis that explicitly contains the solenoidal (loop) functions, the requirement for the remainder of the space cannot be that it should be irrotational, i.e., one cannot resort to Helmholtz decomposition theorem.

This is not necessary, however, because the nonsolenoidal basis functions are defined by the requirement that taken together with the loops, they form a complete basis for the solution space. Stated formally, since the solenoidal part $\underline{J}''$ is the null space of the div operator, the nonsolenoidal basis must be the complement of this null space.

In order to find an explicit expression for the above requirement, one first notes that the new basis functions are combinations of rooftops $\underline{R}_n(\underline{\rho})$, i.e.,

$$\underline{X}_a(\underline{\rho}) = \sum_n x_{na}\underline{R}_n(\underline{\rho}), \quad \underline{L}_a(\underline{\rho}) = \sum_n \ell_{na}\underline{R}_n(\underline{\rho}) \quad (6)$$

so that the solenoidal and nonsolenoidal bases are defined by the rectangular coefficient matrices $[X] = [x_{na}]$ $(N \times N_x)$ and $[L] = [\ell_{na}]$ $(N \times N_\ell)$ that specify the passage from the rooftop basis to the $\underline{L}$ and $\underline{X}$ bases. Otherwise stated, the passage from the rooftop representation ($[I]$) to the representation in the new basis is specified by the $N \times N$ matrix $[T]$

$$[T] = [[X], [L]]. \quad (7)$$

The requirement for the new basis is equivalent to the request that $[T]$ should not be singular.

Having defined all the necessary background, one can now proceed to explicitly determine the basis for the nonsolenoidal part.

B. The Current-Charge Mapping

Since the solenoidal part is div free while the divergence of $\underline{J}'$, $\sigma(\underline{\rho}) = \nabla_t \cdot \underline{J}'$, is not identically vanishing, it is clear that σ will play a key role in defining the basis for $\underline{J}'$. In

the following, σ is called "(surface) charge (distribution)" and denoted by $\sigma(\underline{\rho})$

$$\sigma(\underline{\rho}) = \nabla_t \cdot \underline{J} = \nabla_t \cdot \underline{J}' = \sum_{n=1}^{N} I_n \nabla_t \cdot \underline{R}_n. \tag{8}$$

The correspondence between $\underline{J}'$ and σ will be employed to find a way of specifying the coefficients $[x_{an}]$. To do this, one needs to investigate first how the properties of the rooftop representation translate into those of σ. For currents represented by rooftops, the charge distribution σ is piecewise constant (as $\nabla_t \cdot \underline{R}_n$) and this is the regularity required for the basis functions employed to represent the charge; therefore, the most natural choice for these functions are the pulse functions $p_a(\underline{\rho})$, which are vanishing on all but one cell

$$\sigma(\underline{\rho}) = \sum_a C_a p_a(\underline{\rho}). \tag{9}$$

To find the relationship between the discretized representations of $\underline{J}'$ and σ, (6) and (9) are now substituted into (8) and (8) is tested onto the charge space, i.e., it is projected onto the pulse functions $p_a(\underline{\rho})$; by doing so, from (1) and (8) one obtains

$$[C] = [Q][I], \quad Q_{an} = \langle p_a, \nabla_t \cdot \underline{R}_n \rangle \tag{10}$$

where $[C]$ and $[I]$ are the column vectors of the homonymous coefficients.

Finally, it must also be considered explicitly that any solution $\underline{J}$ to the EFIE, like each of the rooftops, has zero *total* surface charge

$$\int_\Sigma dS\, \sigma(\underline{\rho}) = 0 \tag{11}$$

so that by inserting the representation (9) in (11)

$$\sum_{a=1}^{Nc} C_a K_a = 0, \quad K_a = \int_{\Sigma_a} dS\, p_a(\underline{\rho}) \tag{12}$$

it is clear that with the chosen discretization there are only $N_c - 1$ degrees of freedom for the charge distribution, i.e., there are only $N_c - 1$ independent charge coefficients C_a. Therefore, one needs to consider a charge vector $[c]$ consisting of any $N_c - 1$ elements of $[C]$ or of linear combinations of these elements. Otherwise said, instead of $[Q]$, one considers an $(N_c - 1) \times N$ matrix $[q]$ obtained by deleting any row or linear combination of rows from $[Q]$. As detailed in the Appendix, it can be shown that both $[Q]$ and $[q]$ have rank $N_c - 1$ and, therefore, the $(N_c - 1) \times N$ matrix $[q]$ specifies a full-rank mapping between the N-dimensional space of the rooftop current coefficients $[I]$ and the $(N_c - 1)$-dimensional space of the charge coefficients. As shown in the Appendix, the rank of $[q]$ equals the dimensionality $N_x = N - N_\ell$ of the nonsolenoidal subspace.

It can be further noted that the nullspace of the mapping described by $[q]$ is the space of the coefficients representing solenoidal functions, i.e., (see Appendix)

$$\mathrm{null}([q]) = \mathrm{span}([L_j], j = 1 : N_\ell) \tag{13}$$

or

$$[q][L] = [0]. \tag{14}$$

The above results show that:

1) the matrix $[q]$ is the discretized version of the div operator for currents represented by rooftops and charges represented by pulses;
2) equation (14) specifies the complete orthogonality between the columns of $[q]^T$ and those of $[L]$.

This suggests the use of the charge matrix $[q]$ to construct the nonsolenoidal basis.

C. The Star Basis

Addressing finally the determination of the nonsolenoidal basis, it can be observed that the choice

$$[X] = [q]^T \tag{15}$$

makes the complete transformation matrix $[T]$ in (7) surely nonsingular since

1) $\mathrm{rank}([L]) = N_\ell$, $\mathrm{rank}([X]) = \mathrm{rank}([q]) = N - N_\ell$ (see Appendix);
2) $[L]$ and $[X]$ are orthogonal.

As $x_{na} = q_{an}$ is nonzero only for rooftops extending into the cell a, each function $\underline{X}_a$ is composed of these same rooftops, with a geometrical support that suggests for these basis functions the name of "stars" [4]. An example is shown in Fig. 1 for a rectangular mesh on a rectangular plate; note that because central cells are accessed by four rooftops while border cells only by three or less, the stars "loose their arms" when approaching the edges of Σ. Examples of stars in triangular meshes are shown in [2] and [3] and will not be repeated here.

D. Differential Properties of Stars

1) Irrotational Property: The irrotational property for the surface current $\underline{J}$ has to be understood in a weak sense (almost everywhere) since, as already stated, div-conforming subdomain basis functions cannot be curl conforming [1]. In the present case, the rooftop basis functions have continuous or vanishing normal current across all edges, which makes the divergence (derivative along the current) regular, but the current component parallel to edges does not vanish at the edges and the curl (derivative across the current direction) will exhibit line deltas there. Therefore, contrary to usual statements [3], [10], the star (or "patch") basis functions are not irrotational (curl free). It can be further observed that on an open surface (like in patch antennas), even using infinitely continuous functions (as possible with entire-domain functions on separable simple domains) the solution to EFIE cannot be irrotational in a strong sense since it must be defined over the entire plane; however, generally, vanishing outside the conductors [14] and the current component parallel to edges cannot vanish.

The weak irrotationality of the star-basis functions is now investigated, applying the results in (5) with $\underline{J} = \underline{X}_i$ and

considering the usual testing schemes. This means to investigate on whether there is a class of weighting functions ϕ_k (or of solenoidal functions $\underline{\psi}_k$) for which the stars are weakly irrotational, i.e., for which the inner product in (5) vanishes for all ϕ_k and $\underline{X}_i$. The first natural choice is taking linear interpolating weight functions, i.e., $\phi_k = \Lambda_k$ so that via (3) one has $\underline{\psi}_k = \underline{L}_k$ and the product in (5) is the loop-star projection $\langle \underline{L}_k, \underline{X}_i \rangle$; this choice clearly corresponds to the Galerkin testing scheme for the moment of method (MoM). In this case, it can be remarked that the orthogonality of the loop and star coefficients (14), (15) do not imply orthogonality of these two classes of functions; indeed, denoting by $[X_i]$ the ith column of $[X]$ and by

$$[\Pi^R] = [\Pi^R_{mn}] = [\langle \underline{R}_m, \underline{R}_n \rangle] \tag{16}$$

the projection matrix of the rooftops, one has

$$\langle \underline{L}_k, \underline{X}_i \rangle = [L_k]^T [\Pi^R][X_i] \neq [L_k]^T [X_i] \tag{17}$$

because the rooftops are not an orthogonal basis $\langle \underline{R}_m, \underline{R}_n \rangle \neq \delta_{mn}$. Relaxing the regularity class of the weighting functions ϕ_k, the first step is having piecewise-constant ("pulse") functions that, in turn, correspond to razor-blade testing for the solenoidal weighting $\underline{\psi}_k = \nabla_t \times \hat{n}\phi_k$; consistently with the rooftop representation, one takes this razor blades along the usual center lines of the rooftops [12] that correspond to transforming the surface integral in (5) into a line integral over a closed path passing through the midpoints of all inner edges in a loop function (see [2]). Also in this case the projections between the rooftops and their associated razor blades do not yield a diagonal matrix and, in general, there is no weak irrotationality with respect to this testing. Finally, employing razor-blade functions for ϕ_k, one gets point-matching for $\nabla_t \times \hat{n}\phi$ at the midpoint of the loop inner edges. In this case, one obtains a diagonal projection matrix and if the mesh is uniform (equilateral triangles or square cells), it is the identity matrix. With this testing and on these regular meshes, the star basis is weakly irrotational.

An alternative, less obvious choice is addressed in Section IV-C below.

2) Testing and Divergence: Dually to the loop basis, one would expect that testing a current $\underline{J}$ onto a star yields information of the divergence of $\underline{J}$ over the domain of the star function. To investigate on this, one can form the inner product $\langle \underline{X}_i, \underline{J} \rangle$ and apply (6), (15), (10), and (16), obtaining

$$t_a = \langle \underline{X}_a, \underline{J} \rangle = [q_a][I^{(s)}], \quad [I^{(s)}] \equiv [\Pi^R][I] \tag{18}$$

where $[q_i]$ is the ith row of $[q]$. In (18), t_a is the average div (charge) of the current $[I^{(s)}]$ over the charge cell a, arising from the rooftops extending into cell a, i.e., from the domain of the star centered at a. In turn, since the entries of the jth row of the matrix $[\Pi^R]$ are nonzero for all rooftops overlapping rooftop j, the jth rooftop of current $[I^{(s)}]$ arises from contributions of current $[I]$ on neighboring rooftops; as a result, t_a in (18) is a discretized version of the div operator, but with an averaging over a wider region than would result from normal application to the rooftop basis. This "spreading" property reduces as the testing implied in (18) becomes razor blade or point matching.

IV. Properties of the Loop-Star Basis

A. Isotropic Scalarity

In the presented scheme, the two components of the current (solenoidal and nonsolenoidal) are brought into correspondence with two scalar quantities, the charge σ in (8) and the scalar function M in (2). It is important to note that these two scalar functions have a specified regularity and that this is "isotropic," i.e., independent of the spatial direction. On the contrary, if one employs the x- and y-current components (or any other choice of components of the vector function $\underline{J}$), this property does not hold; for example, for rooftops on a rectangular mesh, the current along x has to be piecewise linear along x and piecewise constant along y. The isotropy of the scalar functions employed here allows one to define basis functions exactly as in a scalar problem.

B. Numerical Properties

The effect of the loop-star decomposition on the numerical solution of the EFIE is now discussed.

The MoM impedance matrix $[Z]_{\rm LS}$ obtained using the loop-star basis can be obtained from the corresponding matrix in the rooftop basis $[Z]_r$, via the (sparse) transformation

$$[Z]_{\rm LS} = [T]^T [Z]_r [T] \tag{19}$$

where, as discussed in Section III, $[T]$ in (7) is block-wise orthogonal. However, the transformation is not globally orthogonal and, therefore, the condition number of the two impedance matrices in the rooftop and loop-star bases will not be the same. As a general remark, loops and stars tend to be independent as the frequency approaches zero [2], [3] and at finite frequencies they retain some degree of independence. As a result, in general, diagonal matrix entries for loops and stars differ significantly in magnitude, and a preliminary balancing is recommendable. The influence on conditioning is discussed in detail in [2] and [3], and the diagonal-dominance (DD) properties are discussed in [2] (and references therein). Here, planar microstrip patch antennas on dielectric substrates have been considered as an example (as in [10]) with a rectangular mesh and employing Galerkin testing. Two cases have been considered: a square electromagnetically coupled patch and a rectangular patch with monolithic recessed feeding. The details of the physical structure and of the discretization are given in [9] and [15]; both cases have been validated against measurement (of the input impedance) or independent solutions, as reported in the references above. The results obtained with the loop-star grouping have been compared to those obtained with the usual rooftop basis; in both reported cases the relative difference between the computed currents is less than 10^{-7} over the entire frequency sweep about the resonance frequency of the considered devices. This is not surprising since problems with the usual rooftops are to be expected in connection with low frequencies, that is, in structures with many basis functions on irregular structures with detail scales significantly smaller than the wavelength. In these cases, the loop-star decomposition fixes the problem. Large differences have instead been reported in [10] for structures of comparable

(resonant) size, but unfortunately, in [10], no indication is given about which solution is to be considered most accurate and no comparison with measurement or literature is presented to resolve the doubt.

As to the conditioning and DD, the results found in the present examples are in agreement with those in [2] and [3]; at these near-resonance frequencies, the loop-star basis is not expected to improve the conditioning and, indeed, in agreement with the results in [2] and [3] the condition number is better in the rooftop basis. However, the loop-star basis introduces a remarkable improvement in terms of DD. The diagonal-dominance ratio (DDR)

$$DDR_i([Z]) = \frac{|Z_{ii}|}{\sum_{j,i\neq j}|Z_{ij}|} \tag{20}$$

controls the convergence of iterative solvers; strict DD, i.e., $DDR_i > 1\ \forall i$, guarantees convergence of Jacobi iterations [2], [16, ch. 10], and the larger the DDR, the faster the convergence. Here, taking as reference a square patch, the DDR in the rooftop basis is always less than one ($\max(DDR_i) = 0.48$), while in the loop-star basis (after balancing), it grows significantly with $\min(DDR_i) = 0.6$ and $\max(DDR_i) = 2.3$.

C. Extension to Irrotational Testing

From the discussion on irrotationality in Section III-D, one also gains insight on whether this property can be achieved by choosing the basis functions. The equivalence of weak irrotationality to orthogonality between the two dual sets of basis functions (loop, star) points at the role of the rooftop projection matrix $[\Pi^R]$ in (17) and by incorporating it into the definition of basis functions the discussed orthogonality can be obtained. Indeed, two "adjoint" dual sets $\{\underline{L}_n^{\perp}, \underline{X}_n^{\perp}\}$ can be defined with coefficients given by

$$[L^{\perp}] = [\Pi^R]^{-1}[L], \quad [X^{\perp}] = [\Pi^R]^{-1}[X] \tag{21}$$

for which it is apparent that $\langle \underline{L}_k^{\perp}, \underline{X}_i \rangle = 0, \langle \underline{L}_k, \underline{X}_i^{\perp} \rangle = 0$; that is, star functions $\underline{X}$ are irrotational if tested upon the "adjoint" solenoidal functions $\underline{L}^{\perp}$ and the "adjoint" star functions $\underline{X}^{\perp}$ are irrotational if tested upon the loop functions $\underline{L}$. Dually, by inserting (1) and (21) into (18), one shows that $\langle \underline{X}_k^{\perp}, \underline{J} \rangle = [q_k]^T[I] = c_k$, i.e., the charge of kth cell.

These adjoint sets can be employed for testing the EFIE, thus obtaining a complete solenoidal-irrotational decomposition of the basis functions. Note that this corresponds to "left-multiplying" the original $[Z]_r$ times $[\Pi^R]^{-1}$; that is, to test the EFIE onto an adjoint set of functions that are biorthogonal with respect to the rooftop-basis functions.

An example of the adjoint star and loop functions is given in Fig. 2; the figure refers to functions located at the center of the mesh in Fig. 1; since the difference between these functions and their star and loop counterparts is difficult to see on an vector plot, Fig. 2 reports the composition of an adjoint loop and an adjoint star in terms of (usual) star and loop functions. From the computational point of view, the matrix $[\Pi^R]$ is highly sparse, symmetric, and positive-definite, so that its inversion is not a problem. However, the feasibility of this testing option depends on whether the coefficient

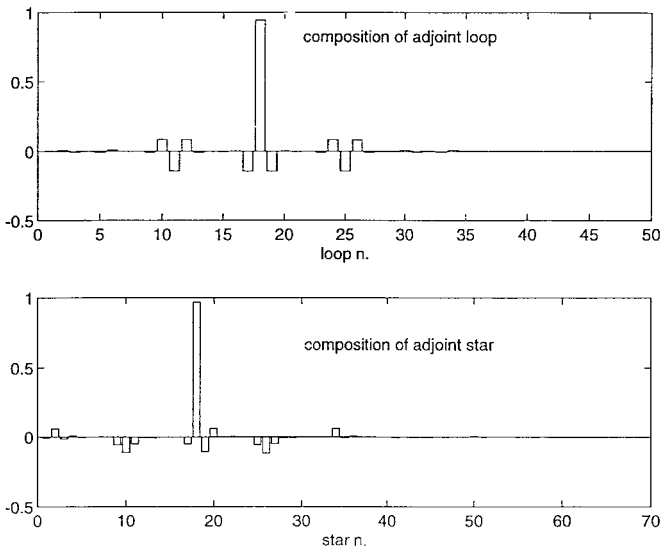

Fig. 2. Representation of adjoint loop and star functions $\underline{L}_n^{\perp}$ and $\underline{X}_n^{\perp}$ in terms of usual loop ($\underline{L}_n$) and star ($\underline{X}_n$) functions. The graphs report the coefficients of the loopand star representation of adjoint functions located at the center ofthe mesh of Fig. 1.

matrices $[L^{\perp}]$ and $[X^{\perp}]$ are sparse or not. This is the case for rectangular meshes, but no guarantee exists of this property on a triangular unstructured mesh.

In any case, weak irrotationality does not appear to give any definite numerical advantage in the solution of the integral equation. In the EFIE, the curl operation does not appear explicitly (as opposed to the div) and one can note that instead, the curl always appears together with some smoothing kernel that filters out the irregularities associated to the curl operation on a correct div-conforming basis (see [7] for the planar case). Therefore, while the solenoidal loop functions disappear from the singular term of the EFIE [7], [10], no such simplification is granted to a weakly irrotational basis.

Finally, using (5) with (17) and (21) along with the definition of $[q]$, one has

$$\begin{bmatrix} [q] \\ [\underline{L}^{\perp}] \end{bmatrix} [I] = \begin{bmatrix} [c] \\ [\mu] \end{bmatrix} \tag{22}$$

where $\mu_k = \langle \Lambda_k, \hat{n} \cdot \nabla_t \times \underline{J} \rangle$ is the curl of $\underline{J}$ averaged over the loop domain, and c_k the div of $\underline{J}$ averaged over the charge cell domain. Inversion of (22) above yields a discretized form of the (surface) Helmholtz representation of $\underline{J}$, i.e., the representation (in a weak sense) of $\underline{J}$ in terms of two scalar functions related to the curl and div. One could think of using such a representation directly into the EFIE (in which the div operation arises explicitly); however, although the matrix on the left-hand side (LHS) of (22) is highly sparse, its inverse is not and this option so far has not been found to be numerically efficient.

V. Summary

A scheme has been proposed for the determination of the basis functions for the solenoidal and nonsolenoidal parts of the surface current, known as "loops" and "stars." The described approach leads to the two classes of basis functions

with operations on "isotropic" *scalar* functions, related to the charge and the normal magnetic current. The properties of the basis functions have been discussed, also showing that they act as div and curl operator when used for testing. The issue of irrotationality of the star function has been addressed, and dual bases have been introduced that render the stars weakly irrotational. The proposed approach allows to show the completeness of the loop-star basis, and the algorithm for the generation of the basis functions is *explicit*.

Although extension to different types of loop- and star-like functions is beyond the scopes of this work, it is believed that the correspondence between star and loop functions and isotropic scalar quantities can be used as a guideline for the generation of more efficient bases, especially of multilevel/multiresolution type, since most literature in this sense is for scalar problems. In addition, the separation of the solution into solenoidal and nonsolenoidal functions is of importance to address the issue of the MoM matrix condition number [7] and a multilevel/multiresolution scheme in this framework shows interesting features [13]. Work in this sense is in progress.

APPENDIX

In this Appendix, it is shown that the rank of the charge matrices $[q]$ is equal to the number of independent charge cells, $N_c - 1$.

Beginning with the most basic case in which $[q]$ is obtained by deletion of any row of $[Q]$, say the kth, one observes that this operation can be written in matrix form via the matrix $[E^{(k)}]$ whose $N_c - 1$ columns are the $N \times 1$ unit vectors $[e_n] = [\delta_{nm}]$ with $n \neq k$

$$[q]^T = [Q]^T [E^{(k)}] \tag{23}$$

since the columns of $[E^{(k)}]$ are orthogonal $\mathrm{rank}([E^{(k)}]) = N_c - 1$.

In the first place, it is necessary to make sure that the above equation correctly specifies the charge representation of any current or, equivalently, that the reduced matrix $[q]$ has indeed rank $N_c - 1$. To do this, one can further note that the nullspace of $[Q]$ is constituted by the vectors $[I]$ representing solenoidal functions; according to the results of Section II-A, one has $\dim(\mathrm{null}([Q])) = N_\ell$. In turn, N_ℓ is related to the number N_c of cells by the Euler–Poincaré theorem [4], stating that $N_\ell + N_c - 1$ is equal to the number of inner edges of the mesh, i.e., the number N of rooftop functions. The relation between the dimension of the nullspace and the rank of a matrix [16, ch. 1], along with $N_\ell = N - N_C + 1$ yields than that $\mathrm{rank}([Q]) = N_c - 1$. Next, one needs to make sure than this rank property carries over onto the $N_c \times N$ reduced matrix $[q]$. This can be done by inserting (8) into the zero total charge condition (11), noting that $\nabla_t \cdot \underline{J}' = \nabla_t \cdot \underline{J}$ ($\underline{J}''$ being solenoidal) and that testing onto p_a is equivalent to integrating over Σ_a. Thus, one finds $\sum_{a=1}^{N_c} \sum_{n=1}^{N} Q_{an} I_n = 0$ and, since this holds for any $\underline{J}$, i.e., for any $[I]$, the above is equivalent to

$$\sum_{a=1}^{N_c} Q_{an} = 0 \quad \forall n = 1, \cdots, N_c, \quad \text{or} \quad [Q]^T [1_{N_c}] = [0]$$
$$[1_{N_c}]^T \equiv [1, 1, \cdots, 1] \tag{24}$$

that is, the sum of all N_c rows of matrix $[Q]$ has to be the null row vector and the $N_c \times 1$ ones vector $[1_{N_c}]$ is in the nullspace of $[Q]^T$. As to the dimension of this nullspace, one notes that the rank of a matrix is invariant upon the transpose operation so that $\mathrm{rank}([Q]^T) = N_c - 1$ and since $[Q]^T$ is $N \times N_c$, then $\dim(\mathrm{null}([Q]^T)) = 1$; therefore, this nullspace is spanned by the ones vector $[1_{N_c}]$ only. By further observing that the $N_c \times 1$ ones vector $[1_{N_c}]$ cannot be represented by any linear combination of $N_c - 1$ unit vectors $[e_n]$, which are the columns of $[E^{(k)}]$, and that $\mathrm{rank}([E^{(k)}]) = N_c - 1$, one concludes that $\mathrm{rank}([q]) = \mathrm{rank}([Q]) = N_c - 1 = N_x$.

The considerations above extend directly to the case in which the matrix $[Q]$ in (23) is substituted for a matrix $[\tilde{Q}] = [F][Q]$, where $[F]$ is any full-rank $N_c \times N_c$ matrix. For example, if the transformation $[F]$ replaces rows k and ℓ with their sum and difference, respectively, subsequent application of (23) to $[\tilde{Q}]$ will delete the sum of rows k and ℓ.

ACKNOWLEDGMENT

The author would like to thank Prof. D. R. Wilton for many interesting discussions on the subject and for some specific suggestions. He would also like to thank Dr. P. Pirinoli, Prof. R. D. Graglia, and Prof. M. Orefice for their careful reading of the manuscript and an anonymous reviewer for having indicated [2] and [3] and for some remarks that have improved the discussion on the nonsolenoidal part.

REFERENCES

[1] R. D. Graglia, D. R. Wilton, and A. F. Peterson, "Higher order interpolatory vector bases for computational electromagnetics," *IEEE Trans. Antennas Propagat.*, vol. 45, pp. 329–342, Mar. 1997.

[2] M. Burton and S. Kashyap, "A study of a recent moment-method algorithm that is accurate to very low frequencies," *ACES J.*, vol. 10, no. 3, pp. 58–68, Nov. 1995.

[3] W. L. Wu, A. Glisson, and D. Kajfez, "A study of two numerical solution procedures for the electric field integral equation at low frequency," *ACES J.*, vol. 10, no. 3, pp. 69–80, Nov. 1995.

[4] D. R. Wilton, "Topological considerations in surface patch and volume cell modeling of electromagnetic scatters," in *URSI Int. Symp. Electromagn. Theory*, Santiago de Compostela, Spain, Aug. 1983, pp. 65–68.

[5] J. R. Mosig and F. E. Gardiol, "General integral equation formulation of microstrip antennas and scatterers," *Proc. Inst. Elect. Eng.*, vol. 132, pt. H, pp. 424–432, Dec. 1985.

[6] D. Sun, J. Manges, X. Yuan, and Z. Cendes, "Spurious modes in finite-element methods," *IEEE Antennas Propagat. Mag.*, vol. 37. pp. 12–24, Oct. 1995.

[7] G. Vecchi, L. Matekovits, P. Pirinoli, and M. Orefice, "A numerical regularization of the EFIE for three-dimensional planar structures in layered media," *Int. J. Microwave Millimeter-Wave Computer-Aided Eng. (Special Issue Frequency Domain Modeling Planar Circuits Antennas)*, vol. 7, no. 6, pp. 410–431, Nov. 1997.

[8] G. Vecchi, P. Pirinoli, L. Matekovits, and M. Orefice, "A numerical regularization of EFIE for printed structures," in *Proc. 25th Eur. Microwave Conf.*, Bologna, Italy, Sept. 1995, pp. 389–393.

[9] G. Vecchi, L. Matekovits, P. Pirinoli, and M. Orefice, "Application of numerical regularization options to the integral-equation analysis of printed antennas," *IEEE Trans. Antennas Propagat.*, vol. 45, pp. 570–572, Mar. 1997.

[10] S. Uckun, T. K. Sarkar, S. M. Rao, and M. Salazar-Palma, "Novel technique for analysis of electromagnetic scattering from miscostrip antennas of arbitray shape," *IEEE Trans. Microwave Theory Tech.*, vol. 45, pp. 485–491, Apr. 1997.

[11] G. Vecchi, P. Pirinoli, L. Matekovits, and M. Orefice, "Hybrid spectral-spatial method for the analysis of printed antennas," *Radio Sci.*, vol. 31, no. 5, pp. 1263–1270, Sept./Oct. 1996

[12] S. M. Rao, D. R. Wilton, and A. W. Glisson, "Electromagnetic scattering by surfaces of arbitrary shape," *IEEE Trans. Antennas Propagat.*, vol. AP-30, pp. 409–418, May 1982.
[13] P. Pirinoli, G. Vecchi, and M. Orefice, "Application of dual wavelet-like functions to the analysis of printed antennas," in *URSI Proc. URSI Int. Symp. Electromagn. Theory*, Thessaloniki, Greece, May 1998, pp. 621–623.
[14] G. Vecchi, P. Pirinoli, and M. Orefice, "On the use of cavity modes as basis functions in the full-wave analysis if printed antennas," *IEEE Trans. Antennas Propagat.*, vol. 46, no. 4, pp. 589–594, Apr. 1998.
[15] G. Vecchi, L. Matekovits, P. Pirinoli, and M. Orefice, "Static extraction, 'static' basis functions and regularization in the analysis of printed antennas," in *Proc. 13th Annu. Rev. Progress Appl. Computat. Electromagn. (ACES)*, Monterey, CA, Mar. 1997, pp. 1523–1530.
[16] G. H. Golub and C. F. Van Loan, *Matrix Computation*. Baltimore, MD: John Hopkins Univ. Press, 1983.

Giuseppe Vecchi (M'90) received the Laurea and Ph.D. (Dottorato di Ricerca) degrees in electronic engineering from Politecnico di Torino, Torino, Italy, in 1985 and 1989, respectively.

He was a Visiting Scientist at Polytechnic University, Farmingdale, NY, from August 1989 to February 1990, when he joined the Politecnico di Torino as a Researcher in the Department of Electronics. In November 1992 he was appointed Associate Professor of Electromagnetics. His main research activities concern analytical and numerical techniques for antennas and circuits and electromagnetic compatibility.